

# Electrochemical Control of Peptide Self-Organization on Atomically Flat Solid Surfaces: A Case Study with Graphite

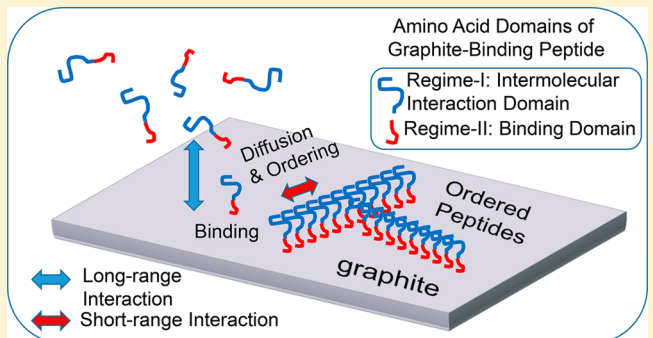
Takakazu Seki,<sup>†,§</sup> Christopher R. So,<sup>‡,§</sup> Tamon R. Page,<sup>†,‡</sup> David Starkebaum,<sup>‡</sup> Yuhei Hayamizu,<sup>†,‡</sup> and Mehmet Sarikaya<sup>\*,‡,§</sup>

<sup>†</sup>Department of Materials Science and Engineering, Tokyo Institute of Technology, Tokyo 152-8550, Japan

<sup>‡</sup>Genetically Engineered Materials Science and Engineering Center, Departments of Materials Science and Engineering and Chemical Engineering, University of Washington, Seattle, Washington 98195, United States

## Supporting Information

**ABSTRACT:** The nanoscale self-organization of biomolecules, such as proteins and peptides, on solid surfaces under controlled conditions is an important issue in establishing functional bio/solid soft interfaces for bioassays, biosensors, and biofuel cells. Electrostatic interaction between proteins and surfaces is one of the most essential parameters in the adsorption and self-assembly of proteins on solid surfaces. Although the adsorption of proteins has been studied with respect to the electrochemical surface potential, the self-assembly of proteins or peptides forming well-organized nanostructures templated by lattice structure of the solid surfaces has not been studied in the relation to the surface potential. In this work, we utilize graphite-binding peptides (GrBPs) selected by the phage display method to investigate the relationship between the electrochemical potential of the highly ordered pyrolytic graphite (HOPG) and peptide self-organization forming long-range-ordered structures. Under modulated electrical bias, graphite-binding peptides form various ordered structures, such as well-ordered nanowires, dendritic structures, wavy wires, amorphous (disordered) structures, and islands. A systematic investigation of the correlation between peptide sequence and self-organizational characteristics reveals that the presence of the bias-sensitive amino acid modules in the peptide sequence has a significant effect on not only surface coverage but also on the morphological features of self-assembled structures. Our results show a new method to control peptide self-assembly by means of applied electrochemical bias as well as peptide design—rules for the construction of functional soft bio/solid interfaces that could be integrated in a wide range of practical implementations.



## INTRODUCTION

Interfaces between proteins and solid surfaces have been widely studied in many fields, such as biofuel cells,<sup>1</sup> biomedical devices for immunoassay,<sup>2</sup> biominerilization,<sup>3</sup> drug delivery,<sup>4</sup> biosensors,<sup>5–7</sup> and protein arrays for proteomics.<sup>8</sup> Among many possible approaches, direct self-organization of proteins on solid surfaces is a promising candidate for constructing well-controlled versatile interfaces with tailored structures of proteins. Proteins have been studied to form a facile interface for more stable and sensitive biosensors.<sup>9–11</sup> Numerous proteins have been demonstrated to form ordered structures on the nanoscale.<sup>12</sup> As an alternative to these proteins, peptides have recently become ubiquitous molecular building blocks in the design and controlled formation of the interfaces.<sup>13,14</sup> A variety of designed peptides have shown self-assembly into ordered structures on graphite and mica.<sup>15–18</sup> Peptides selected by display libraries have also been demonstrated to form ordered structures on gold<sup>19</sup> and graphite surfaces.<sup>20</sup> More recently, several studies have demonstrated the self-assembly of peptides on single-layer graphene.<sup>18,21,22</sup> The behavior of these

peptides on solid surfaces has also been investigated theoretically using computational modeling.<sup>22–25</sup>

In this work, we utilized graphite-binding peptides (GrBPs), which were originally selected by phage display method, that display a specific binding affinity to cleaved graphite surface.<sup>20</sup> These peptides form long-range-ordered nanostructures with 6-fold symmetry on the atomically flat graphite (0001) surface, indicating the recognition of the graphite crystal lattice. The peptide sequence contains two important domains: a solid-binding domain and an intermolecular interactive domain. The binding domain contains two tyrosines (at positions 9 and 12) contributing to the  $\pi-\pi$  interaction with the graphite surface. The intermolecular interactive domain contains hydrophobic (4–8) and hydrophilic (1–3) amino acids, forming an amphiphilic sequence. Simple replacements of one or more amino acids in the sequence cause major binding and

Received: June 29, 2017

Revised: August 21, 2017

Published: October 2, 2017



morphological changes in the peptide nanostructures that subsequently form on the surface. In all cases, mono-molecular-thick nanostructures are generated, either in the form of a confluent film covering the whole surface or nanowires and nanoislands.<sup>20</sup> Furthermore, it has also been shown that the mutations of these peptides have the ability to create nanostructures on other layered materials with atomically flat surfaces, such as MoS<sub>2</sub> and BN.<sup>22</sup> These observations suggest that partial changes in the sequence affect the fundamental surface processes of the peptides, i.e., binding, diffusion, and interactions among the peptides, leading eventually to the formation of ordered structures.

In an attempt to develop an external means to regulate the surface morphology of peptides, electrochemical control of the surface charge by an applied voltage appears to be a favorable way to control the behavior of the peptide on the surface. So far, there have been many studies on protein adsorption controlled through the electrochemical approach.<sup>26,27</sup> However, to the best of our knowledge, there is no experimental investigation for the electrochemical control of the long-range-ordered self-organization of proteins or peptides on atomically flat solid surfaces. In this work, we have investigated the correlation of peptides sequences to their response of the electrochemically applied surface potential in their organization on the solid surface toward achieving potential design rules. In particular, the net charge of the peptide and the position of the charged amino acids in the sequence, whether in the intermolecular interaction domain or in the surface-binding domain, were interrogated on the surface behavior of peptides in forming ordered or disordered structures.

As schematically shown in Figure 1, we consider two important interactions during the processes of peptide self-

peptide/peptide interaction on the surface ( $I_{pp}$ ) for aggregation or ordering (regime II). The above interactions presumably contain a combination of (i) long-range interactions, i.e., electrostatic forces and templating by the solid, and (ii) short-range interactions, i.e., van der Waals forces, salt bridges, and hydrogen bonding. The question here is how the surface potential affects these surface phenomena through the modulation of these interactions by mutating the peptide at specific positions in the sequence.

To address this question, we utilized wild type (WT) GrBPS and its variants (M6, M8, M9, and N-WT), as shown in Table 1. These peptides were rationally designed as having net negative (WT and M6), positive (M8), and neutral (M9 and N-WT) charges based on their expected values at neutral pH. In the original (WT) sequence, two carboxylic acid side chains (glutamic acid and aspartic acid) are located in the middle of the peptide, in the domain that is dominant in peptide–peptide interactions. In the M6 variant, these two acidic (negatively charged) residues were moved in between the two aromatic tyrosine residues near the C-terminus. Because these tyrosines are attributed to binding sites for graphite, we expect enhanced interactions between the charged amino acids with the solid surface. In the M8 variant, the two carboxylic acids in M6 were replaced with two alkaline (positively charged) arginine residues. In the M9 variant, the two acidic residues in the WT peptide were replaced with their noncharged amide equivalents (glutamic acid to glutamine, aspartic acid to asparagine). Finally, in the N-WT variant, one acidic residue was replaced with an alkaline residue (glutamic acid to lysine) to form a net-neutral zwitterionic peptide at neutral pH. We subsequently investigated the effects of electrochemical bias on the process of binding and organization of these peptide variants on the cleaved graphite surface.

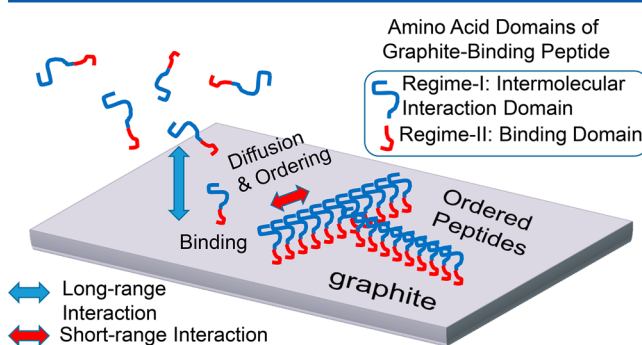


**Figure 1.** Schematic illustration depicting interactions during the peptide self-organization process on the solid surface. Regimes I and II show two main processes: (I) solid binding and (II) diffusion and ordering.

organization on the solid surface: (1) peptide/surface interaction ( $I_{ps}$ ) for binding and diffusion (regime I) and (2)

## MATERIALS AND METHODS

**Experimental Condition for Peptide Self-Assembly.** To investigate the electrochemical effect, we used a simple electrochemical cell with highly ordered pyrolytic graphite (HOPG) as the working electrode and a Pt wire as the counter electrode (Figure 2a). The HOPG substrate (SPI-1) was purchased from the SPI supplies. Peptide solution was prepared by dissolving a lyophilized peptide powder in Milli-Q water. First, we placed a droplet of peptide solution (30  $\mu$ L) on the freshly cleaved HOPG substrate, and a Pt electrode was immediately inserted into the droplet. Then, a constant voltage was applied between the substrate and the Pt electrode. The sample was incubated at room temperature for 1 h under a humidified atmosphere to prevent the evaporation of the droplet. After incubation, the droplet was gently blown off with nitrogen gas, and any remaining water was evaporated by continuous blowing with dry nitrogen gas for about 20 s.

**Atomic Force Microscopy.** After the samples were dried, the morphology of self-organized peptides on HOPG was characterized by atomic force microscopy (AFM). AFM measurements were carried out

**Table 1. Sequences of Peptide Mutations Used in This Work**

name	amino acid sequence												MW	charge
	1	2	3	4	5	6	7	8	9	10	11	12		
GrBPS(WT)	I	M	V	T	E	S	S	D	Y	S	S	Y	1381.4	-2
GrBPS(M6)	I	M	V	T	A	S	S	A	Y	D	D	Y	1335.4	-2
GrBPS(M8)	I	M	V	T	A	S	S	A	Y	R	R	Y	1417.6	+2
GrBPS(M9)	I	M	V	T	Q	S	S	N	Y	S	S	Y	1379.5	0
neutral-WT (N-WT)	I	M	V	T	K	S	S	D	Y	S	S	Y	1380.5	0

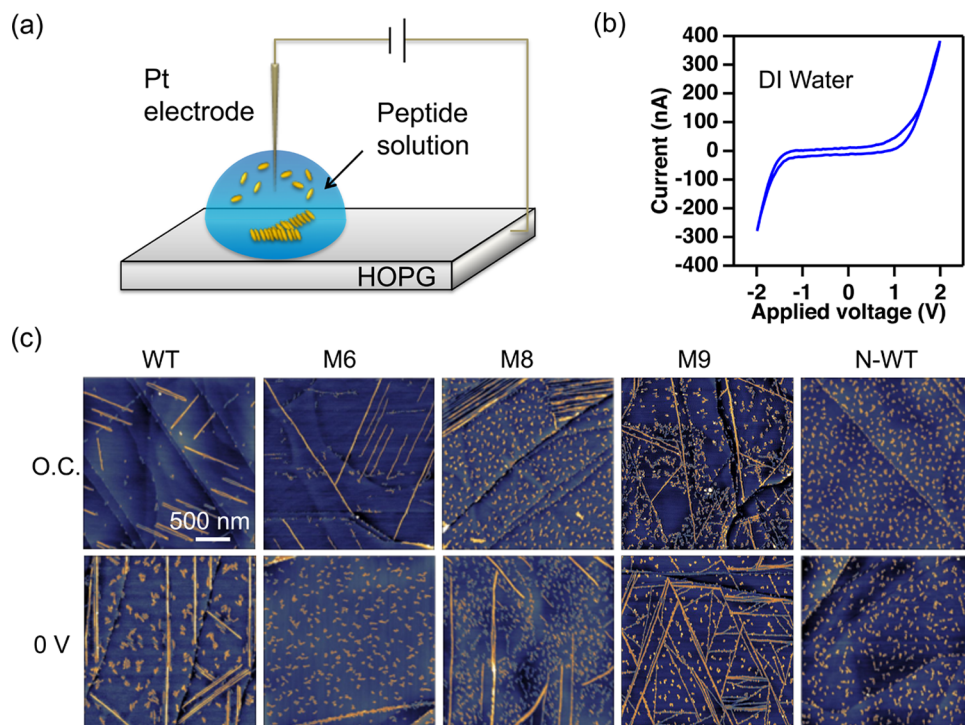


**Figure 2.** (a) Experimental setup for the electrochemical control of peptide self-assembly on the graphite surface. The setup is composed of freshly cleaved HOPG, a potentiostat, and a Pt electrode. (b) Cyclic voltammetry behavior of the HOPG/DI water/Pt system with a voltage sweep rate of 10 mV/s. (c) AFM images of the peptide organizations under open circuit (OC) and 0 V conditions with a peptide concentration of 0.1  $\mu$ M in each case. AFM images were recorded under dry conditions after blowing with nitrogen.

with a 5500 AFM from Keysight Technologies. The cantilever used in this work was an OMCL-AC160TS from Olympus.

**Cyclic Voltammetry.** Cyclic voltammetry was carried out with a Versastat3 from Princeton Applied Research. On the basis of a cyclic voltammetry (CV) measurement (Figure 2b), the current between the Pt electrode and the HOPG remained within the range of  $\pm 20$  nA as long as the voltage was kept between  $-1.0$  and  $+0.5$  V. In this range, the electrochemical interface works as a capacitor as a result of the negligible current through the solution. Thus, we utilized this range to change the surface potential of the HOPG substrate in a controlled manner.

## RESULTS AND DISCUSSIONS

Before applying an electrochemical bias to the substrate, we first examined the self-organization of each peptide incubated for 1 h on HOPG without connecting the electrode with graphite (OC). Focusing on initial binding of peptides to the graphite surface, we utilized a peptide solution with a low concentration of 0.1  $\mu$ M to limit probable peptide collisions on the surface as much as possible. In the previous report,<sup>20</sup> it was found that this low concentration allows the WT peptide to form isolated islands or clusters on the surface instead of the ordered nanostructures formed at higher concentrations.

AFM measurements of HOPG samples incubated in 0.1  $\mu$ M WT, M6, M8, M9, and N-WT reveal surface coverages of 36, 14, 48, 23, and 17%, respectively (Figure 2c). This indicates a significant effect of the peptide sequences on their binding affinity to the surface. Following the open circuit experiment, we performed the incubation of peptides with the Pt electrode at zero voltage (closed circuit). The self-organized structures of all peptides revealed similar morphological features to those obtained under open circuit conditions (Figure 2c). The similarity probably arises from their similar surface potentials in each case. The open circuit voltage of the Pt/water/HOPG

system was  $-0.23$  V, which is close to 0 V (Supporting Info, Figure S1).

Next, we found that the peptides' response to applied voltages differed depending on the net charge in each peptide sequence (Figure 3). From AFM measurements carried out using a low concentration of peptides, i.e., 0.1  $\mu$ M, we obtained the coverage of peptides depending on the applied voltage and identified three different groups in the trend of the peptide coverage as the voltage was swept from  $-1.0$  to  $0.5$  V. While negatively charged peptides (WT and M6) monotonically increase their coverage, positively charged peptide (M8) decreases its coverage. The surface coverages of WT, M6, and M8 were modulated from 12, 6, and 35% to 24, 24, and 15%, respectively, with the increase in the applied voltage from  $-1$  V to  $+0.5$  V. On the other hand, two neutral peptides (M9 and N-WT) show constant coverage throughout the range of applied voltage. These results can be simply explained by electrostatic attractive or repulsive forces, which can be proportionally changed with the change in the surface potential. The charged peptides can be affected by the surface potential through the electrostatic force interaction with the surface, leading to the variation in the flux of peptides from the solution to the surface. On the contrary, the neutral peptides were not affected by the surface potential. Interestingly, M9, containing no charged amino acid, displays morphological features over the applied voltages with an almost constant coverage. Although dotlike structures were observed at a voltage of more than 0 V, wirelike structures were observed under 0 V, i.e., the tendency to form peptide nanowires. In the absence of the change in the surface coverage, sufficient molecular surface diffusion of peptides is necessary to form nanowires, i.e., long-range organized structures. This analysis may require that the

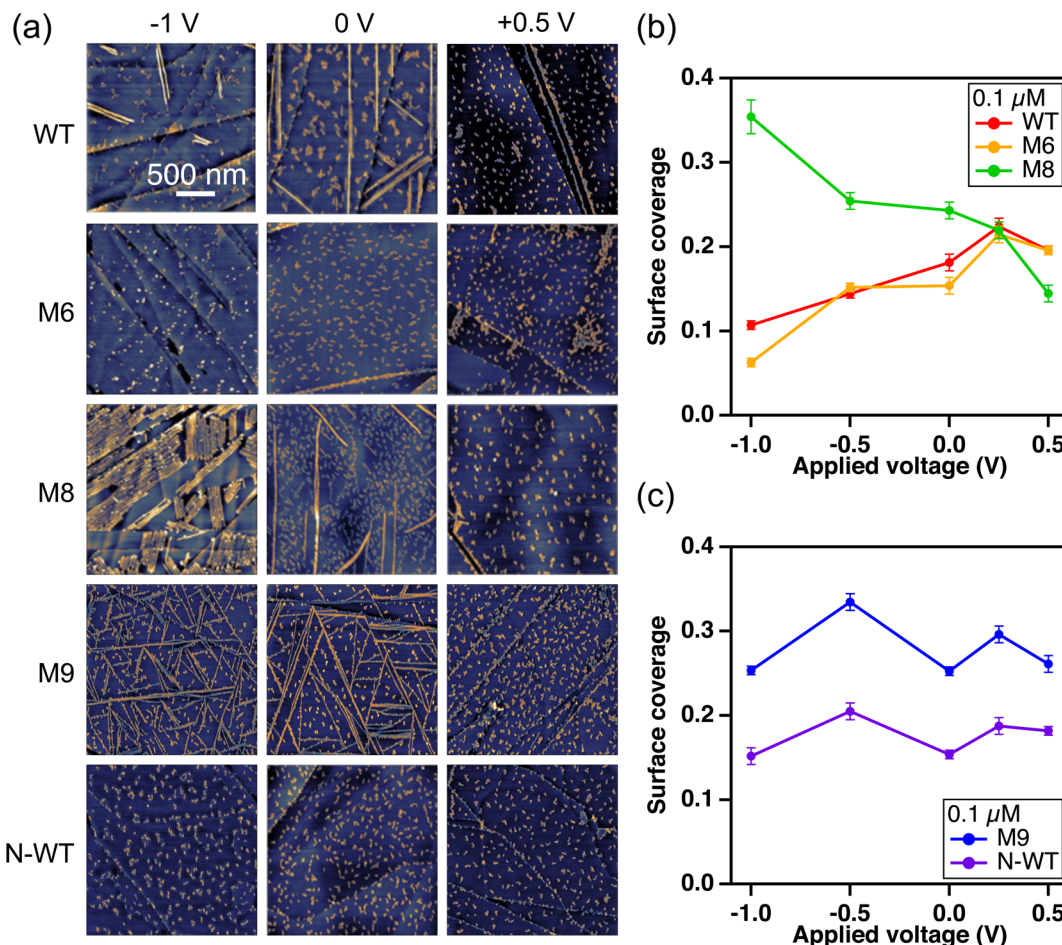


**Figure 3.** (a) AFM height images of peptide organization upon applying voltage from  $-1.0$  to  $+0.5$  V at a low flux rate (low concentration of  $0.1\ \mu\text{M}$ ). The color bar range of images is  $3\ \text{nm}$ . All AFM images were recorded under dry conditions. The AFM images (b and c) represent the surface coverage of peptides vs applied voltage.

processes of peptide binding and diffusion were strongly enhanced by increasing the surface potential.

For further investigation into the morphological response to the applied bias, a higher concentration ( $1.0\ \mu\text{M}$ ) of peptides was utilized. Centering on the effect of charges in the sequence, negatively charged peptides (WT and M6) and positively charged peptide (M8) were studied here. In contrast to low-concentration experiments where peptide interactions on the surface were limited, it is expected that intermolecular interactions among the peptides could play a more significant role with a higher peptide concentration in the solution exposed to the solid surface. Indeed, AFM observations revealed more complex morphological changes in response to the applied voltage than the ones at low concentration (Figure 4). First, WT and M6 displayed significant morphological differences regardless of having the same net charge. In the range of  $-1.0$  to  $-0.5$  V, WT formed a dendritic structure. Although WT and M6 show well-ordered structures in the form of more straight, robust nanowires at  $0\ \text{V}$ , WT lacks linearity in the self-organized structure and display wavy structure at positive bias. The M6 peptide, however, appears to form well-ordered structures through the voltage range used.

The morphological characteristics of the M8 variant are significantly different than those seen with the M6 variant under these bias conditions. Although well-ordered structures form at large negative bias at  $-1\ \text{V}$ , this significantly changes at

$-0.5\ \text{V}$  bias, and the nanowire structure further breaks down at  $0\ \text{V}$ , long-range order disappears, and the peptides form only disordered structure at  $+0.5\ \text{V}$ . (See also the associated fast Fourier transforms in the insets showing the breakdown of the long-range ordering of the peptides on the surface in this case.) Another interesting observation is that the well-ordered domains have coarser feature sizes, i.e., domains being wider and longer, for M6 while the feature sizes are smaller in M8.

The domain structure and the behavior of the long-range-ordered structures of M6 and M8 are understood by considering the affinity of the peptides for the surface involving electrostatic interaction, especially when the charged amino acids are in the binding domain. Because of electrostatic interactions, the increased flux of the peptides to the surface then is likely to increase the nucleation density of the peptide clusters. Although M6 and M8 have opposite signs of charge, the electrostatic force on the surface increases when an electrical bias is applied to HOPG. Furthermore, the peptide is not likely to diffuse on the surface, resulting in the formation of many domains with finer dimensions.

The behavior of M9, the neutral peptide, is quite different from that of all of the other peptides in that the surface coverage is highest among all and the ordered structures with relatively smaller domains persist up until the bias becomes positive. Both the flux of the peptide striking and sticking to the surface and its diffusion on the surface result in a large area of

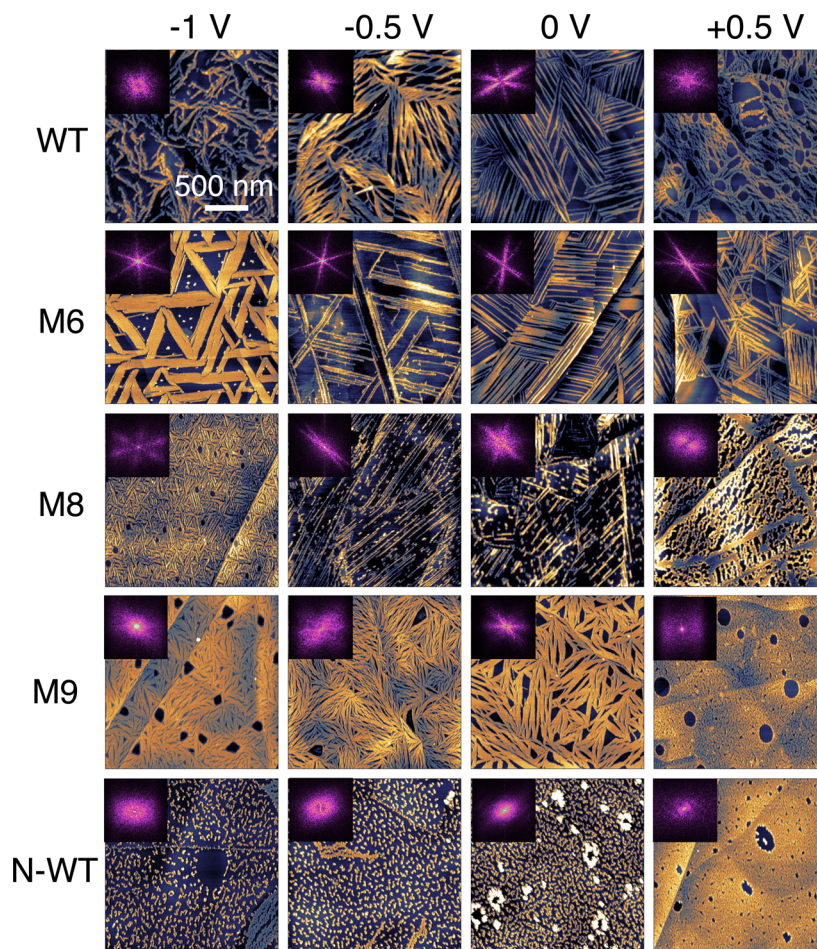


**Figure 4.** AFM images of self-organization behavior of the peptides at various applied voltages with a peptide concentration of  $1 \mu\text{M}$ . The inset in each image is the FFT pattern corresponding to the assembly of the specific peptide under the bias shown. All AFM images were recorded under dry conditions.

coverage. When the positive bias is applied, the surface coverage is almost complete, but without the ordered structure. This may be due to the large flux of peptides immobilized on the surface with less opportunity to diffuse, refold, and interact with neighboring peptides to form solid-induced ordering.

The behavior of charge-neutral peptide N-WT is also interesting in that it never forms ordered structures on the surface and that the surface coverage is slightly increased over the bias range from  $-1$  to  $0$  V. When the bias becomes positive, the surface coverage is similar to the M9 case. N-WT never shows ordered domains or linear structures but displays randomly oriented short, linear clusters. This behavior of the peptides forming disordered structures throughout the whole bias range may be due to the zwitterionic nature of the N-WT. This tendency has been found in the other type of peptides, which is experimentally selected as a gold-binding peptide, AuBP1. This dodecapeptide has also a zwitterionic nature and does not have the ability to form ordered structures on a graphite surface (*Supporting Information*, Figures S2 and S3).

It is important reemphasize that the size of the ordered domains and the nanowires has a tendency to respond to the applied voltage in all cases, in particular, in the cases of M6 and M8. According to a general concept of surface molecular assembly, the size of molecular aggregates on a surface can be inversely increased to the flux rate of the adsorbates: a lower flux rate causes a larger domain size.<sup>28</sup> Our observation exactly

follows this tendency, which could result from the variation in the flux rate controlled by the applied voltage. To the best of our knowledge, this is the first demonstration of controllable peptide self-organization into ordered structures by electrochemical methods. The electrochemical control of the flux rate can be useful in defining nanostructures of self-assembled peptides, especially in forming long and thin well-ordered nanostructures (*Supporting Information*, Figure S4).

Next, we evaluated the correlation of coverage vs applied voltage from the AFM observations. Obviously, the result with the high concentration did not show a monotonic modulation of coverage by the voltage in all cases (*Figure 5a*). Here, we have identified three groups of peptides according to their response to the applied bias: (group i) WT, (group ii) M6 and M8, and (group iii) M9 and N-WT. Group I shows small variations in coverage over the range of applied voltage. This is likely due to the reasons that the binding strengths and surface diffusion rates of the peptides do not change but the molecular interactions do change, leading to the differences in ordering behavior of the peptides. Group ii shows high coverage at large voltages ( $-1$  and  $0.5$  V) but low coverage at small voltages ( $-0.5$  and  $0$  V). Group iii shows an increase in coverage in the range of positive applied voltages. These tendencies can be closely related to the net charge of each peptide depending on their local pH in the vicinity of the graphite surface. In *Figure 5b*, we have plotted the net charge of each peptide at different

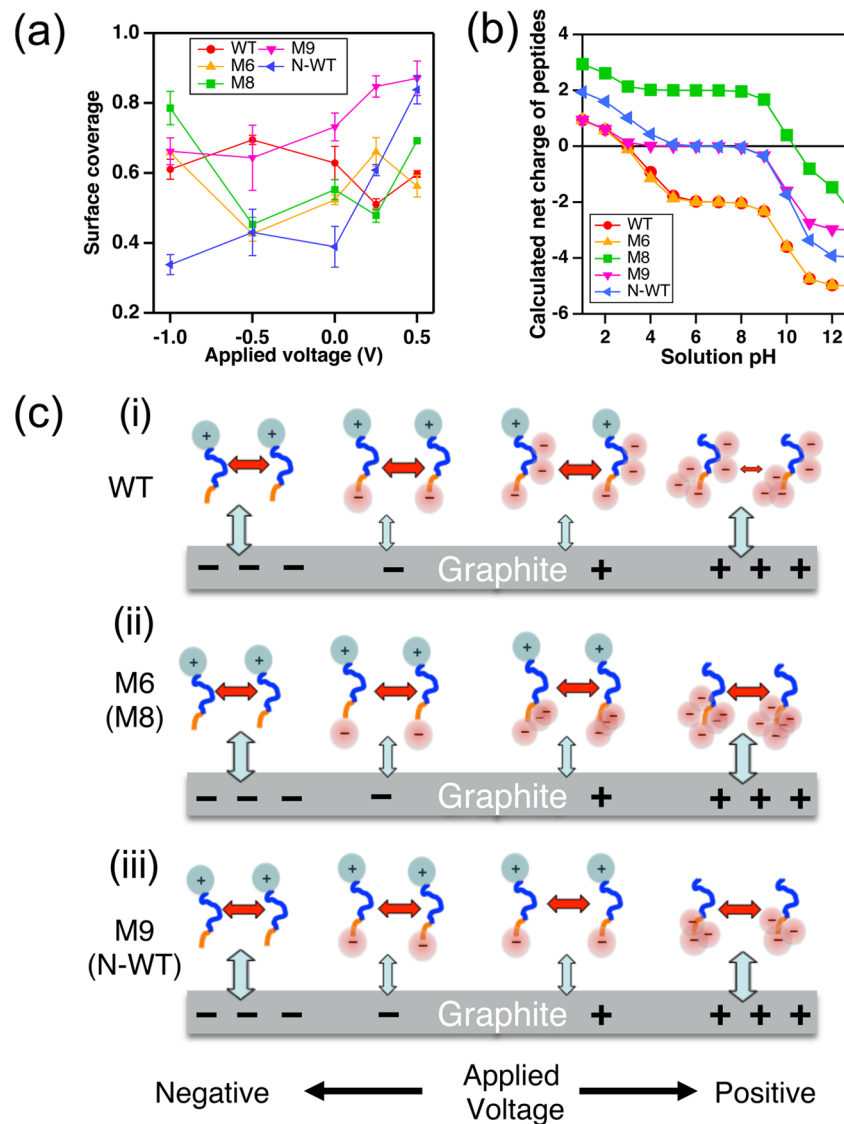


**Figure 5.** (a) Plot of the coverage of each peptide vs the applied voltage. (b) Calculated net charge of peptides at various pH values. (c) Schematics showing charges of peptides at various applied voltages. Red and blue arrows indicate intermolecular interactions between the peptides ( $I_{pp}$ ) and the peptide/surface ( $I_{ps}$ ) interactions, respectively.

pH on the basis of the  $pK_a$  of each amino acid in the peptide sequence.<sup>26</sup> The charge of the peptides with solution pH clearly shows that there are three types of behavior corresponding to the groups discussed above: negative, positive, and neutral peptides in the range of pH from 5 to 9. In our experiment, the peptide aqueous solution is under an equilibrium condition in air. Thus, the pH value of the bulk solution was most likely 5.7. Because of the protonation or deprotonation of residues and termini, all of the peptides change their net charges. The local pH on the graphite surface can vary with the applied voltage. Previous work reported the local pH of water in the vicinity of a metal surface and proposed an equation,  $\text{pH} = 7 \pm 7.83 \text{ V}$ , where V is the voltage applied to the metal surface.<sup>29</sup> On the basis of this, roughly speaking, the local pH controlled in this work can be estimated to be from  $-1.73$  to  $11.4$ , which covers most of the range in Figure 5b. The net charge probably affects both the intermolecular interaction among the peptides ( $I_{pp}$ ) and the peptide/solid surface interactions ( $I_{sp}$ ).

Finally, to explain the morphology formed and the coverage observed for each of the peptides over the range of applied

voltages, we provide Figure 5c, which shows our hypothesis on the interactions of the three categories of the peptides at various surface potentials. Here, we focus on the kinetics of peptide self-assembly on the HOPG surface. The coverage of peptides or the growth rate of the peptide nanostructures can be related to the relative values of  $I_{pp}$  and  $I_{sp}$ , where larger  $I_{pp}$  and  $I_{sp}$  contribute to a higher coverage. The difference between groups I and ii can be explained by the position of charged amino acids. For WT, the first eight amino acids have an amphiphilic nature, and they have been considered to play an important role in the intermolecular interactions between peptides ( $I_{pp}$ ), leading to the long-range ordering of the peptides. On the basis of this concept, it is reasonable to assume that  $I_{pp}$  may be suppressed for the WT-peptides at high voltages as a result of a repulsive Coulombic force caused by high net charges among peptides. Interestingly, WT is the only peptide that does not show a clear increase in coverage at high voltage. On the other hand, M6 and M8 peptides have charged amino acids in the binding domain. Thus, these peptides may have a dominant contribution of  $I_{sp}$  to the final coverage, where

the net charge varying with the local pH has repulsive or attractive force, respectively, on the graphite surface depending on the surface charge. At 0.5 V, the pH may reach the point where both tyrosines and the N-terminus can be deprotonated. This charge regulation probably causes strong binding to the surface, resulting in a high coverage without linear well-ordered nanostructures. Thus, although peptides in group iii do not have a net charge at pH7, the coverage increases at 0.5 V as well. It is worth mentioning that all of the peptides start losing their ability to form well-ordered structures at 1.0 V (*Supporting Information*, Figure S5), although some (M8, M9, and N-WT) reach this at 0.5 V. This may be caused by the hydrolysis of peptides under such a strong alkaline condition. In the discussion above, we considered the kinetics of the system without taking into account the possible variations of the local pH on the surface. The local pH can vary self-consistently by the presence of the bound peptide nanostructures on the surface with a high coverage density. For further understanding, it will be necessary to establish a self-consistent computational approach in the future.

In conclusion, we have successfully established conditions in which one can tune the morphological features of peptide self-organization on a graphite substrate by adjusting the electrochemically applied bias. At a low concentration of peptides (0.1  $\mu\text{M}$ ), the surface coverage of charged peptides (WT, M6, and M8) was monotonically modulated by the applied bias. Charge-neutral peptides (M9 and N-WT), however, were mostly insensitive to the applied voltage. At a high concentration (1.0  $\mu\text{M}$ ), self-organized peptides displayed well-ordered structures. The size of the peptide nanostructures has been controlled by the applied voltage, most probably resulting from the tuning of the flux rate of peptides by the surface potential of graphite, affecting both the surface nucleation rate and the growth rate. However, N-WT peptides with a zwitterionic nature exhibited only shorter nondescript linear aggregates without the ability to form ordered structures. For a further understanding of the surface process of peptides, further experimental and computational modeling studies at the molecular level will be required. The molecular conformation can be tightly correlated to the controlled surface potential, resulting in changes in surface phenomena including the binding, diffusion, and self-assembly of peptides into various nanostructures and their morphological behavior. The electrochemical control presented in this work could allow one to design and construct peptide-based nanoscale biomolecular scaffolds on the graphite surface for future biosensing and bioelectronics applications. Furthermore, temporal control of the surface potential may become a new tool for studying the dynamic control of molecular conformations of peptides in forming ordered nanostructures, a key concept that may be extended to tailored protein assembly forming soft interfaces on solid-state devices.<sup>22</sup>

## ■ ASSOCIATED CONTENT

### § Supporting Information

The Supporting Information is available free of charge on the ACS Publications website at DOI: [10.1021/acs.langmuir.7b02231](https://doi.org/10.1021/acs.langmuir.7b02231).

Open circuit voltage measurement, analysis of peptide nanostructures, comparison with other peptides, and AFM images at 1 V ([PDF](#))

## ■ AUTHOR INFORMATION

### Corresponding Author

\*E-mail: [sarikaya@uw.edu](mailto:sarikaya@uw.edu).

### ORCID iD

Mehmet Sarikaya: [0000-0003-3856-6360](#)

### Author Contributions

The concept of extraneous fields affecting peptide assembly on atomically flat surfaces was conceived by Y.H. and M.S. The experiments were carried out by T.S., C.R.S., T.R.P., D.S., and Y.H. Y.H. prepared the draft, all authors made corrections, and M.S. finalized the manuscript.

### Author Contributions

<sup>§</sup>These authors contributed equally.

### Notes

The authors declare no competing financial interest.

## ■ ACKNOWLEDGMENTS

The research was supported (D.S., T.R.P., and M.S.) by the USA-NSF through the DMREF program (DMR-1629071) at the UW's GEMSEC, Genetically Engineered Materials Science and Engineering Center. C.R.S. was partially supported by NCI training grant T32CA138312. Y.H. was supported by the JST PRESTO programs and the Tokyo Tech Tenure Track System. T.S. and Y.H. were supported by JSPS KAKENHI grants 25706012, 16H05973, and 15H04192. The work was carried out at GEMSEC-SECF, a member of the Materials Facilities Network of MRSEC, and at Y.H.'s facilities at Tokyo Tech.

## ■ REFERENCES

- (1) Halámková, L.; Halámek, J.; Bocharova, V.; Szczupak, A.; Alfönta, L.; Katz, E. Implanted biofuel cell operating in a living snail. *J. Am. Chem. Soc.* **2012**, *134* (11), 5040–5043.
- (2) Seidel, M.; Niessner, R. Automated analytical microarrays: a critical review. *Anal. Bioanal. Chem.* **2008**, *391* (5), 1521–1544.
- (3) Lowenstam, H. A.; Weiner, S. *On Biomineralization*; Oxford University Press: New York, 1989.
- (4) Monopoli, M. P.; Walczyk, D.; Campbell, A.; Elia, G.; Lynch, I.; Baldelli Bombelli, F.; Dawson, K. A. Physical-chemical aspects of protein corona: relevance to in vitro and in vivo biological impacts of nanoparticles. *J. Am. Chem. Soc.* **2011**, *133* (8), 2525–2534.
- (5) Khatayevich, D.; Page, T.; Gresswell, C.; Hayamizu, Y.; Grady, W.; Sarikaya, M. Selective Detection of Target Proteins by Peptide-Enabled Graphene Biosensor. *Small* **2014**, *10* (8), 1505–1513.
- (6) Page, T. R.; Hayamizu, Y.; So, C. R.; Sarikaya, M. Electrical detection of biomolecular adsorption on sprayed graphene sheets. *Biosens. Bioelectron.* **2012**, *33* (1), 304–308.
- (7) Ohno, Y.; Maehashi, K.; Matsumoto, K. Label-free biosensors based on aptamer-modified graphene field-effect transistors. *J. Am. Chem. Soc.* **2010**, *132* (51), 18012–18013.
- (8) Colwill, K.; Gräslund, S.; Group, R. P. B. W.. A roadmap to generate renewable protein binders to the human proteome. *Nat. Methods* **2011**, *8* (7), 551–558.
- (9) Katz, E. Application of bifunctional reagents for immobilization of proteins on a carbon electrode surface: oriented immobilization of photosynthetic reaction centers. *J. Electroanal. Chem.* **1994**, *365* (1–2), 157–164.
- (10) Chen, R. J.; Zhang, Y.; Wang, D.; Dai, H. Noncovalent sidewall functionalization of single-walled carbon nanotubes for protein immobilization. *J. Am. Chem. Soc.* **2001**, *123* (16), 3838–3839.
- (11) Rusmini, F.; Zhong, Z.; Feijen, J. Protein immobilization strategies for protein biochips. *Biomacromolecules* **2007**, *8* (6), 1775–1789.
- (12) De Yoreo, J. J.; Chung, S.; Friddle, R. W. In Situ atomic force microscopy as a tool for investigating interactions and assembly

dynamics in biomolecular and biomineral systems. *Adv. Funct. Mater.* **2013**, *23* (20), 2525–2538.

(13) Whaley, S. R.; English, D.; Hu, E. L.; Barbara, P. F.; Belcher, A. M. Selection of peptides with semiconductor binding specificity for directed nanocrystal assembly. *Nature* **2000**, *405* (6787), 665–668.

(14) Sarikaya, M.; Tamerler, C.; Jen, A. K.-Y.; Schulten, K.; Baneyx, F. Molecular biomimetics: nanotechnology through biology. *Nat. Mater.* **2003**, *2* (9), 577–585.

(15) Kowalewski, T.; Holtzman, D. M. In situ atomic force microscopy study of Alzheimer's  $\beta$ -amyloid peptide on different substrates: New insights into mechanism of  $\beta$ -sheet formation. *Proc. Natl. Acad. Sci. U. S. A.* **1999**, *96* (7), 3688–3693.

(16) Zhang, F.; Du, H. N.; Zhang, Z. X.; Ji, L. N.; Li, H. T.; Tang, L.; Wang, H. B.; Fan, C. H.; Xu, H. J.; Zhang, Y. Epitaxial growth of peptide nanofilaments on inorganic surfaces: Effects of interfacial hydrophobicity/hydrophilicity. *Angew. Chem., Int. Ed.* **2006**, *45* (22), 3611–3613.

(17) Mao, X.-B.; Wang, C.-X.; Wu, X.-K.; Ma, X.-J.; Liu, L.; Zhang, L.; Niu, L.; Guo, Y.-Y.; Li, D.-H.; Yang, Y.-L. Beta structure motifs of islet amyloid polypeptides identified through surface-mediated assemblies. *Proc. Natl. Acad. Sci. U. S. A.* **2011**, *108* (49), 19605–19610.

(18) Mustata, G.-M.; Kim, Y. H.; Zhang, J.; DeGrado, W. F.; Grigoryan, G.; Wanunu, M. Graphene symmetry amplified by designed peptide self-assembly. *Biophys. J.* **2016**, *110* (11), 2507–2516.

(19) So, C. R.; Kulp, J. L., III; Oren, E. E.; Zareie, H.; Tamerler, C.; Evans, J. S.; Sarikaya, M. Molecular recognition and supramolecular self-assembly of a genetically engineered gold binding peptide on Au {111}. *ACS Nano* **2009**, *3* (6), 1525–1531.

(20) So, C. R.; Hayamizu, Y.; Yazici, H.; Gresswell, C.; Khatayevich, D.; Tamerler, C.; Sarikaya, M. Controlling self-assembly of engineered peptides on graphite by rational mutation. *ACS Nano* **2012**, *6* (2), 1648–1656.

(21) Kim, S. N.; Kuang, Z.; Slocik, J. M.; Jones, S. E.; Cui, Y.; Farmer, B. L.; McAlpine, M. C.; Naik, R. R. Preferential binding of peptides to graphene edges and planes. *J. Am. Chem. Soc.* **2011**, *133* (37), 14480–14483.

(22) Hayamizu, Y.; So, C. R.; Dag, S.; Page, T. S.; Starkebaum, D.; Sarikaya, M. Bioelectronic interfaces by spontaneously organized peptides on 2D atomic single layer materials. *Sci. Rep.* **2016**, *6*, 33778.

(23) Cohavi, O.; Corni, S.; De Rienzo, F.; Di Felice, R.; Gottschalk, K. E.; Hoefling, M.; Kokh, D.; Molinari, E.; Schreiber, G.; Vaskevich, A. Protein–surface interactions: challenging experiments and computations. *J. Mol. Recognit.* **2009**, *23* (3), 259–262.

(24) Akdim, B.; Pachter, R.; Kim, S. S.; Naik, R. R.; Walsh, T. R.; Trohalaki, S.; Hong, G.; Kuang, Z.; Farmer, B. L. Electronic properties of a graphene device with peptide adsorption: insight from simulation. *ACS Appl. Mater. Interfaces* **2013**, *5* (15), 7470–7477.

(25) Hughes, Z. E.; Tomásio, S. M.; Walsh, T. R. Efficient simulations of the aqueous bio-interface of graphitic nanostructures with a polarisable model. *Nanoscale* **2014**, *6* (10), 5438–5448.

(26) Hartvig, R. A.; van de Weert, M.; Østergaard, J.; Jorgensen, L.; Jensen, H. Protein adsorption at charged surfaces: the role of electrostatic interactions and interfacial charge regulation. *Langmuir* **2011**, *27* (6), 2634–2643.

(27) Kubiak-Ossowska, K.; Mulheran, P. A. Mechanism of hen egg white lysozyme adsorption on a charged solid surface. *Langmuir* **2010**, *26* (20), 15954–15965.

(28) Barth, J. V.; Costantini, G.; Kern, K. Engineering atomic and molecular nanostructures at surfaces. *Nature* **2005**, *437* (7059), 671–679.

(29) Morrow, R.; McKenzie, D. The time-dependent development of electric double-layers in pure water at metal electrodes: the effect of an applied voltage on the local pH. *Proc. R. Soc. London, Ser. A* **2012**, *468*, 18–34.